HHS Public Access

Author manuscript

Nat Commun. Author manuscript; available in PMC 2015 October 24.

Published in final edited form as:

Nat Commun. ; 6: 6910. doi:10.1038/ncomms7910.

DNMT1 is essential for mammary and cancer stem cell maintenance and tumorigenesis

Rajneesh Pathania[1], **Sabarish Ramachandran**[1], **Selvakumar Elangovan**[1], **Ravi Padia**[1], **Pengyi Yang**[2], **Senthilkumar Cinghu**[2], **Rajalakshmi Veeranan-Karmegam**[1], **Pachiappan Arjunan**[1], **Jaya P. Gnana-Prakasam**[1], **Sadanand Fulzele**[3], **Lirong Pei**[4], **Chang-Sheng Chang**[4], **Hyeon Choi**[5,6], **Huidong Shi**[1,6], **Santhakumar Manicassamy**[6], **Puttur D. Prasad**[1,6], **Suash Sharma**[4,6], **Vadivel Ganapathy**[1,6], **Raja Jothi**[2], and **Muthusamy Thangaraju**[1,6,*]

[1]Department of Biochemistry and Molecular Biology, Medical College of Georgia, Georgia Regents University, Augusta, GA, USA

[2]System Biology Section, Epigenetics & Stem Cell Biology Laboratory, National Institute of Environmental Health Sciences, National Institutes of Health, Research Triangle Park, NC, USA

[3]Department of Orthopedic Surgery, Medical College of Georgia, Georgia Regents University, Augusta, GA, USA

[4]Department of Pathology, Medical College of Georgia, Georgia Regents University, Augusta, GA, USA

[5]Department of Biostatistics, Medical College of Georgia, Georgia Regents University, Augusta, GA, USA

[6]Department of Cancer Research Center, Medical College of Georgia, Georgia Regents University, Augusta, GA, USA

Abstract

Mammary stem/progenitor cells (MaSCs) maintain self-renewal of the mammary epithelium during puberty and pregnancy. DNA methylation provides a potential epigenetic mechanism for maintaining cellular memory during self-renewal. Although DNA methyltransferases (DNMTs) are dispensable for embryonic stem cell maintenance, their role in maintaining MaSCs and cancer stem cells (CSCs) in constantly replenishing mammary epithelium is unclear. Here we show that DNMT1 is indispensable for MaSC maintenance. Furthermore, we find that DNMT1 expression is elevated in mammary tumors, and mammary gland-specific *DNMT1* deletion protects mice from mammary tumorigenesis by limiting the CSC pool. Through genome-scale methylation studies,

[*]**Requests for reprints:** Muthusamy Thangaraju, Ph. D., Department of Biochemistry and Molecular Biology, Medical College of Georgia, Georgia Regents University, Augusta, GA 30912. Phone: 706-721-4219; mthangaraju@gru.edu.

Author contribution: R. P. and M. T. designed experiments and analyzed the data; R. P. performed most of the experiments; H. S., J-H. C. and C-S. C. conducted bioinformatics analyses; L. P. and C-S. C. prepared the library for DNA methylation analysis; S. R., S. E. and R. P. contributed to mouse xenograft studies; R.V-K. performed western blots; P. A. and J. P. G. performed 5-mCy assays; S. F and S. M. helped in the isolation of mammary stem cells; P. D. P. and S. S. contributed to tumor morphometric analysis; P. Y., S. C. and R.J. analyzed the histone methylation data; R. P., R. J., V. G. and M. T. wrote the manuscript.

Competing financial interests: All authors declare no competing financial interests.

we identify *ISL1* as a direct DNMT1 target, hypermethylated and downregulated in mammary tumors and CSCs. DNMT inhibition or ISL1 expression in breast cancer cells limits CSC population. Altogether, our studies uncover an essential role for DNMT1 in MaSC and CSC maintenance and identify DNMT1-ISL1 axis as a potential therapeutic target for breast cancer treatment.

INTRODUCTION

Mammary epithelium undergoes multiple rounds of proliferation, differentiation and apoptosis during pregnancy, lactation and involution[1,2]. Classical transplantation assays, lineage tracing, and cell-fate mapping studies in mice have revealed the existence of a hierarchy of stem and progenitor cells among the mammary epithelium[3,4], with a considerable increase in mammary stem cell (MaSC) activity during pregnancy[5]. Given the increased risk of breast cancer associated with pregnancy in the short term, the augmented MaSC pool has been postulated to be the cellular basis for increased breast cancer incidence during pregnancy[5].

The maintenance of stem/progenitor cells and their differentiation fate in the mammary epithelium follows a well-defined epigenetic program, with a growing number of chromatin regulators implicated in controlling the homeostatic balance between self-renewal and differentiation state[6,7]. DNA methylation is among the best studied epigenetic modification[8], which provides a potential mechanism for maintaining cellular memory during repeated cell divisions[9]. Embryonic stem cells (ESCs) that lack DNA methyltransferases are viable, but die when induced to differentiate[10–12], suggesting that proper establishment and maintenance of DNA methylation patterns are essential for mammalian development and for the normal functioning of the adult organism[13]. Indeed, a growing number of human diseases including cancer have been found to be associated with aberrant DNA hypermethylation at CpG islands, most of which are unmethylated in normal somatic cells[13]. Since de novo methylation of CpG islands is widespread in tumor cells and is an early event in transformation[14,15], it represents an excellent biomarker for early cancer detection[16].

DNA methyltransferase 1 (Dnmt1) is essential for the maintenance of hematopoietic stem/progenitor cells[17], epidermal progenitor cells[18], mesenchymal stem cells[19], and leukemia stem cells[20], but its role in the regulation of mammary stem/progenitor cells and mammary tumorigenesis has not been studied. Here we show that Dnmt1 is required for mammary gland outgrowth and terminal end bud development and that mammary-gland specific *Dnmt1* deletion in mice leads to significant reduction in mammary stem/progenitor cells. We also show that *Dnmt1* deletion or inhibition of Dnmt1 activity almost completely abolishes Neu-Tg- and C3(1)-SV40-Tg- driven mammary tumor formation and metastasis, a phenomenon that is associated with significant reduction in cancer stem cells (CSCs). Through genome-scale DNA methylation studies in normal and CSCs, we find *ISL1*, an endogenous inhibitor of estrogen receptor-driven transcription activation[21], is hypermethylated in CSCs and silenced in most human breast cancers. Functional re-expression of ISL1 or inhibition of DNMT activity in breast cancer cells reduces cell

growth, migration, and CSC formation. Our studies provide the first *in vivo* evidence showing a requirement for DNMT1 in mammary stem/progenitor cell and CSC maintenance, and identify DNMT1-ISL1 axis as a potential therapeutic target for breast cancer treatment.

RESULTS

Dnmt1 expression during mammary gland development

We investigated *Dnmt1* expression during different stages of mammary gland development and observed significantly higher levels of Dnmt1 expression in mid-pregnant mammary gland (Fig. 1a–c) along with a dramatic increase in stem cell-enriched basal cells ($Lin^{-}CD49f^{high}CD24^{+}$) and luminal cells ($Lin^{-}CD49f^{low}CD24^{+}$) (Fig. 1d–e). Isolation of $Lin^{-}CD49f^{high}CD24^{+}$ and $Lin^{-}CD49f^{low}CD24^{+}$ cells from 8-week-old virgin mammary glands revealed that both cell populations expressed similar levels of Dnmt1 (Supplementary Fig. 1a–c). To determine the role of *Dnmt1* in the regulation of mammary stem/progenitor cells, we generated mammary gland-specific conditional *Dnmt1*-knockout mice as global deletion of *Dnmt1* leads to early embryonic lethality[11]. We bred mice in which loxP sites flanked exons 4 and 5 of *Dnmt1* gene[11] with mice expressing Cre recombinase under the control of MMTV promoter. *Dnmt1*-deletion in the mammary gland was confirmed by the loss of Dnmt1 expression and significant reduction in DNA methylation levels (Supplementary Fig. 1d–h). To evaluate Dnmt1's role in mammary epithelium, we analyzed mammary glands from wild-type ($Dnmt1^{fl/fl}$) and *Dnmt1*-knockout ($Dnmt1^{\Delta/\Delta}$) female littermates by whole-mount analysis. At 7 weeks postpartum, mammary ducts colonize ~55–60% of the fat pad in $Dnmt1^{fl/fl}$ mice, and terminal end buds (TEBs) that contain stem cells and their highly proliferative progeny extend beyond the lymph nodes (Fig. 1f, g). In contrast, the development of the mammary gland in $Dnmt1^{\Delta/\Delta}$ littermates was severely inhibited. In the mammary gland, a subpopulation of cells located in the basal layer of terminal end ducts has been implicated as stem cells. We found that deletion of *Dnmt1* severely affected TEB development in the virgin mammary glands (Fig. 1h, i).

Dnmt1 is indispensable for mammary stem cell maintenance

To understand the role of *Dnmt1* in the development of mammary gland cellular lineages, we prepared single cell suspensions from mammary glands isolated from $Dnmt1^{fl/fl}$ and $Dnmt1^{\Delta/\Delta}$ female mice. Flow cytometry analysis showed that *Dnmt1* deletion decreased mammary stem cells (MaSCs)-enriched basal cells ($Lin^{-}CD49f^{high}CD24^{+}$) and luminal cells ($Lin^{-}CD49f^{low}CD24^{+}$) (Fig. 2a). Further analysis of the luminal cells using the CD61 marker, which distinguishes between luminal progenitor cells ($Lin^{-}CD49f^{low}CD61^{+}$, ER negative) and mature luminal cells ($Lin^{-}CD49f^{low}CD61^{-}$, ER positive), revealed a significant decrease in luminal progenitors (Fig. 2b). This decrease in MaSCs and progenitor cells is consistent with low mammosphere formation (Fig. 2c) and Ki67 expression (Fig. 1i), and low frequency of mammary repopulating unit (MRU) in $Dnmt1^{\Delta/\Delta}$ mice compared to $Dnmt1^{fl/fl}$ mice (Supplementary Fig. 2). Together, these observations show that Dnmt1 plays a key role in mammary gland development and that deletion of *Dnmt1* severely disrupts TEB development that grows out from MaSCs.

Dnmt1 expression is high in cancer stem cells

DNMT1 is essential for maintaining epidermal progenitor cells by suppressing differentiation[18] and plays a direct role in the self-renewal of hematopoietic stem cells (HSCs) and their commitment to lymphoid lineages[22]. While HSC self-renewal is abrogated by conditional gene knockout of *Dnmt1*, the mature differentiated hematopoietic lineage is unaffected[17,23]. Furthermore, cancer cells maintain stem cell-like gene expression program with differential methylation pattern[24]. However, the expression status of DNMT1 in normal MaSCs and cancer stem cells (CSCs) has not been well studied. Thus, we examined Dnmt1 expression in mammospheres, enriched with stem/progenitor cells, obtained from normal mouse mammary glands, and tumorospheres, enriched with tumor propagating CSCs, obtained from premalignant and tumor tissues of MMTV-Neu mice. We found that CSCs have higher levels of Dnmt1 expression compared with MaSCs, along with higher levels of *Id-1*, an inhibitor of differentiation, and lower levels of β-*casein*, a differentiation marker (Supplementary Fig. 3a, b).

Dnmt1 deletion suppresses mammary tumorigenesis

Several lines of evidence implicate DNA methylation in cancer pathogenesis[25,26], with changes in DNA methylation patterns found to contributing to oncogenesis by affecting the expression levels of proto-oncogenes and tumor-suppressor genes[14,27]. DNA hypomethylation promotes increased expression of oncogenes, whereas DNA hypermethylation silences tumor-suppressor genes[14]. However, there is no direct evidence that either mechanism is operative in mammary tumorigenesis. To test the relative contribution of Dnmt1 in mammary tumorigenesis, we crossed *Dnmt1*$^{\Delta/\Delta}$ mice with MMTV-Neu-Tg mice, which mimic human luminal progenitor cell of origin[28], and C3(1)-SV40-Tg, which mimic human basal triple-negative breast cancer[29]. Over 85% of *Dnmt1*-mutant mice were resistant to Neu-Tg- and C3(1)-SV40-Tg-driven mammary tumor and lung metastasis. About 65% of *Dnmt1*$^{fl/fl}$-MMTV-Neu-Tg mice developed mammary tumor at an average age of 290 days whereas only 12% of *Dnmt1*$^{\Delta/\Delta}$-MMTV-Neu-Tg mice developed mammary tumor at an average age of 360 days (Fig. 3a, b). The tumors developed in Dnmt1$^{\Delta/\Delta}$-MMTV-Neu-Tg mice were smaller in size, less invasive and unable to metastasize to distant organs like lungs (Fig. 3c, d and Supplementary Fig.3c). The overall survival rate of Dnmt1$^{\Delta/\Delta}$-MMTV-Neu-Tg mice was significantly high compared to Dnmt1$^{fl/fl}$-MMTV-Neu-Tg mice (Fig. 3e). Similar results were observed for *Dnmt1*$^{\Delta/\Delta}$-C3(1)-SV40-Tg mice (Fig. 3a, b, d–f and Supplementary Fig. 3d, e).

To test whether the reduced tumor incidence observed in *Dnmt1*-knockout mice is simply due to lower number of epithelial cells that are subjected to transformation, we prepared mammosphere from premalignant mammary glands obtained from *Dnmt1*$^{fl/fl}$-MMTV-Neu-Tg and *Dnmt1*$^{\Delta/\Delta}$-MMTV-Neu-Tg mice, dissociated mammosphere into single cell suspension, and injected the same number (1×10^4) of single cell suspension into NOD/SCID mice. *Dnmt1*-knockout significantly reduced tumor incidence, tumor size, and tumorosphere forming capability (Supplementary Fig.3f–h). These data indicate that delayed tumorigenesis in *Dnmt1*-knockout is not due to lower number of epithelial cells subject to transformation.

Next, we analyzed CSC population in tumor tissues of wild-type and *Dnmt1*-knockout MMTV-Neu and C3(1)-SV40-Tg mice using CD24 and CD49f as a CSC marker[30]. *Dnmt1* deletion significantly limits the CSC-enriched cell fraction (Fig. 3g, h), which is consistent with Dnmt1 activity required for proper renewal of leukemia stem cell[22]. Together, these results suggest that Dnmt1 plays a key role in regulation of CSC self-renewal in mammary epithelium and that functional deletion of this gene protects mice from mammary tumorigenesis by blocking CSC formation.

Inhibition of DNMT activity suppresses mammary tumorigenesis

To test whether pharmacological inhibition of DNMTs will block spontaneous mouse mammary tumorigenesis by inhibiting CSC formation, we implanted a sustained slow releasing DNMT inhibitor 5-azacytidine (5-AzaC) into 12-week-old MMTV-Neu-Tg mice. We also tested the efficacy of HDAC inhibitor butyrate (But) along with 5-AzaC. After confirming reduced DNMT and HDAC activities in cells treated with 5-AzaC and But respectively (Fig. 4a–b), we inspected their tumorosphere forming capabilities. 5-AzaC implantation alone significantly reduced tumorosphere formation, mammary tumorigenicity and metastasis, and accompanied increased overall survival (Fig. 4c–f). The combination of DNMT and HDAC inhibitors greatly enhanced the effect (Fig. 4g). As expected, 5-AzaC implantation significantly reduced CSC formation. Interestingly, analysis of CSCs in mice that had not developed tumors in the presence of 5-AzaC and/or But showed three distinct cell populations, stem ($CD49f^{high}CD24^{+}$), luminal ($CD49f^{low}CD24^{+}$), and stromal ($CD49f^{-}CD24^{-}$) cells, instead of a single CSC population ($CD49f^{+}CD24^{+}$) observed for tumor tissues of untreated control mice (Fig. 4h, top panels). A few animals that were treated with 5-AzaC and/or But developed tumors and these tumors had relatively more CSCs ($CD49f^{+}CD24^{+}$) compared to untreated controls (Fig. 4h, bottom panels) suggesting that tumor cells that are resistant to 5-AzaC and But might undergo other undefined epigenetic changes that could play a role in CSC regulation.

Isl1 is hypermethylated and downregulated in mammary tumors

To gain insight into the mechanism by which DNMTs regulate MaSCs and CSCs, we generated genome-scale methylation profiles[31,32] using reduced representation bisulfite sequencing of genomic DNA isolated from mammospheres, obtained from normal mouse mammary glands, and tumorospheres, obtained from tumor tissues of MMTV-Neu-Tg mice. We identified 2341 differentially methylated regions (DMRs) that were either hypermethylated or hypomethylated in tumorospheres compared with mammospheres (Fig. 5a, Supplementary Fig. 4a–c and Supplementary Data 1). A vast majority of DMRs are hypermethylated in tumorospheres (Supplementary Fig. 4d), which is consistent with the higher levels of Dnmt1 in tumorospheres (Supplementary Fig. 3a, b). Notably, genes associated with hypermethylated CpGs in tumorospheres harbor bivalent histone modifications (activating H3K4me3 and repressive H3K27me3) in MaSCs and luminal progenitors (Supplementary Fig. 4e), which is consistent with previous reports showing that bivalent genes are often found to be DNA-hypermethylated in cancers and that bivalency may predispose tumor suppressor and pro-differentiation genes for later DNA hypermethylation[33].

To identify functional targets of Dnmt1, we focused on 321 genes that are hypermethylated in tumors (Fig. 5b and Supplementary Data 2 and 3). Among the genes are known tumor suppressor genes *Wnt5a*, *Abi3*, and *Tcf7*, and *Isl1*, whose gene product is known to interact with estrogen receptor (ER)[21] (Fig. 5b and Supplementary Fig. 5a–f). Consistent with hypermethylation, gene expression analysis revealed a significant downregulation of these genes in CSC-enriched tumorospheres (Fig. 5b and Supplementary Fig. 5g). WNT5A is known to be silenced in human breast cancer, and loss of WNT5A is associated with early relapse of invasive breast cancer, increased metastasis, and poor survival[34]. Similarly, TCF7 is also known to be silenced in breast cancer, with Tcf7-null mice developing spontaneous mammary adenomas[35]. ABI3 expression is frequently lost or reduced in invasive cancer. Ectopic expression of ABI3 inhibits metastasis and cell migration[36] but ABI3's mechanism of action is not fully understood. Isl1, a transcription factor, is required for the generation of motor neurons[37] and is a marker for a cardiac progenitor cell lineage that is capable of differentiating into three different cell types of the heart: smooth muscle, cardiomyocytes, and endothelial cell types[38]. Isl1 is also known to inhibit ER-driven transcription activation by preventing its dimerization[21]. Given that ERs are overexpressed in ~70% of breast cancer cases, referred to as "ER-positive", we sought to investigate the functional link between Isl1 and breast cancer using human and mouse primary breast tumor tissues and human breast cancer cell lines.

ISL1 expression negatively correlates with DNMT1 expression

Isl1, bivalent in embryonic stem cells (ESCs) and MaSCs (Fig. 5c), is hypermethylated in CSC-enriched tumorspheres (Fig. 5d). Examination of the TCGA and UCSC Cancer Genomics Database reveal that *ISL1* is hypermethylated in a majority of breast cancer subtypes (Fig. 6a). Gene expression data from TCGA Pan-cancer shows that *ISL1* expression is lost or down-regulated in many human cancers, and is negatively correlated with the expression of *DNMT*s in breast cancer (Supplementary Fig. 6a, b). Interestingly, *ISL1* inactivation is not a common phenomenon in all human cancers; its expression is elevated in some human cancers including pancreatic and prostate cancers (Supplementary Fig. 6a), suggesting that the tumor suppressor function of ISL1 is tissue and context dependent.

Using the Gene Set Analysis-Cell line application, we investigated *ISL1* mRNA expression levels across the breast cancer cell line panel and found that *ISL1* is downregulated in a vast majority of breast cancer cell lines (Supplementary Fig. 6c). To confirm these data, we analyzed *ISL1* expression in human primary breast tumor samples and adjacent normal human breast tissue. While *ISL1* transcript level is detectable in normal breast tissues, irrespective of the ER status, *ISL1* level is nearly undetectable in tumor samples (Fig. 6b). Similarly, irrespective of the ER status, ISL1 expression is low to undetectable in most of the human breast cancer cell lines (Fig. 6c and Supplementary Fig. 6d). In addition, examination of *Isl1* expression in control and tumor tissues of four different mouse mammary tumor models (MMTV-PyMT-Tg, MMTV-Hras-Tg, MMTV-Neu-Tg, and C3(1)-SV40-Tg) revealed relatively low levels of Isl1 in mouse mammary tumor tissues compared with the control tissue (Supplementary Fig. 6e, f). Altogether, these results suggested a potential role for ISL1 in suppression of mammary tumorigenesis.

ISL1 expression in cancer cells limits CSC population

To determine whether the silencing of *ISL1* in breast cancer cells is due to DNA-hypermethylation, we treated CAL51 and MB231 cells with DNMT inhibitor 5-AzaC and HDAC inhibitor Valproic acid and found that both inhibitors reactivate *ISL1* expression in these cells (Supplementary Fig. 7a, b). To study the functional implications of ISL1 in breast cancer, we stably expressed ISL1 in CAL51 cells using a lentiviral vector. After confirming the expression of ISL1 in the stable cell clones (Fig. 6d and Supplementary Fig. 7c, d), we investigated the effects of ISL1 expression on cell growth and differentiation, apoptosis, and cell migration. Stably expressed ISL1 in cancer cells significantly reduced cell growth and migration, with a significant induction of apoptosis and differentiation (Fig. 6e–g and Supplementary Fig 7e, f). To gain insight into ISL1's role in the regulation of stem cells, we examined the $CD44^{+}CD24^{-}$ cell population in CAL51-ISL1 stable cells and found that ISL1 expression significantly reduced CSC population (Fig. 6h, i and Supplementary Fig 7g). Together, these data suggest that DNA-hypermethylation is one of the causes, if not the cause, for epigenetic silencing of *ISL1* in breast cancer cells. Consistent with this conclusion, examination of Isl1 expression in mammosphere derived from the mammary glands of $Dnmt1^{fl/fl}$ and $Dnmt1^{\Delta/\Delta}$ mice revealed significantly elevated levels of Isl1 expression in *Dnmt1*-knockout mice (Fig. 6j).

Association between ISL1 expression and overall survival

Finally, to explore the relationship between ISL1 and clinical prognosis, we evaluated the prognostic value of ISL1 in a large clinical microarray database of breast cancer that includes data from 4,142 patients[39]. We found that irrespective of the ER status, low ISL1 expression is associated with poor prognosis and reduced overall survival (Fig. 7) suggesting that ISL1, in addition to its role in the inhibition of estrogen signaling[21], may have other roles in blocking mammary tumorigenesis and progression.

DISCUSSION

In this study, we identified a novel role for Dnmt1 in regulating mammary gland development and mammary stem and progenitor cell maintenance. We found that the *Dnmt1*-knockout ductal epithelium failed to invade the fat pad and mostly resembled the rudimentary mammary tree that is laid down during embryogenesis, indicating an essential role for Dnmt1 in maintaining the myoepithelial stem cell and luminal progenitor lineage in the postnatal mammary gland development. Mammary stem and progenitor cell populations are significantly reduced in *Dnmt1*-knockout mouse, suggesting a critical role for Dnmt1 in mammary stem and progenitor cell expansion and maintenance. MaSCs proliferate and differentiate during pregnancy and lactation and interact with stromal cells and extracellular matrix to sustain normal morphogenesis[6]. In the mammary gland, a subpopulation of cells located in the basal layer of terminal end ducts has been implicated as stem cells. We found that deletion of *Dnmt1* severely affected TEB development, consistent with reduced number of MaSCs. Together, our data support the conclusion that Dnmt1 is essential for MaSC maintenance. Our findings are in line with recent studies showing a requirement for Dnmt1 is the maintenance of hematopoietic stem/progenitor cells[17], epithelial stem cells[18] and mesenchymal stem cells[18].

Our studies in tumor models provide strong evidence for Dnmt1 playing a critical role in mammary tumor growth and progression. Several lines of evidence implicate DNA methylation in cancer pathogenesis[25,26] with changes in DNA methylation patterns contributing to oncogenesis by affecting the expression levels of proto-oncogenes and tumor-suppressor genes[13,14,27]. DNA hypomethylation has been shown to promote increased expression of many oncogenes, while DNA hypermethylation has been shown to silence tumor-suppressor genes[14]. Our studies in human and mouse breast cancer cells show that Dnmt1 deletion decreases tumor formation and metastasis by affecting the self-renewal and proliferation of cancer initiating cells. Moreover, administration of 5-azaC and butyrate during premalignant stage efficiently blocked mammary tumorigenesis and reduced tumorosphere forming potential of CSCs. Together, these results support the conclusion that Dnmt1 is essential for the maintenance of CSCs, which is consistent with a previous study demonstrating an essential role for Dnmt1 in the self-renewal and maintenance of leukemia stem cells[22].

Consistent with the elevated levels of DNMT1 expression in human and mouse cancer cells, a vast majority of differentially methylated regions in tumorospheres are hypermethylated compared to mammospheres. Among the hypermethylated genes are known tumor suppressor genes (*Wnt5a*, *Abi3*, and *Tcf7*) and *Isl1*, whose gene product is a known inhibitor of estrogen receptor-driven transcription activation. *ISL1* is hypermethylated and downregulated in a majority of breast cancer subtypes, with its expression status negatively correlating with DNMT1 expression. Stable expression of ISL1 or inhibition of DNMT activity successfully limited cellular proliferation and CSC fraction. Together, these data support an essential role for Dnmt1 in tumorigenic phenotype of CSCs, and show that inhibition of DNMT activity reverses the abnormal self-renewal properties of CSCs.

In summary, our studies provide the first *in vivo* evidence that DNMT1 is indispensable for MaSC and CSC maintenance and that functional inactivation of this gene drastically reduces mammary tumor formation even in the aggressive triple-negative breast cancer subtype. Our results establish ISL1 hypermethylation status as a potential prognostic marker for early breast cancer diagnosis and a role for DNMT1-specific inhibitors in the eradication of CSCs and associated disease recurrence.

METHODS

Animals

FVB/NJ (Stock # 001800), C57BL/6 (Stock # 000664), MMTV-Neu-Tg (Stock # 002376) NOD.Cg-*Prkdcscid Il2rgtm1Wjl*/SzJ (Stock #00557) and C3(1)-SV40-Tg (Stock # 013591) mice were obtained from Jackson laboratories. All these mice were bred and maintained in Georgia Regents University Animal Facility in accordance with the guidelines of the Institutional Animal Care Use Committees.

Collection of mammary glands

To collect mammary glands from virgin mice, females at approximately 12 weeks of age without any copulation were used. To collect mammary gland from pregnant mice, females

were bred at approximately 8 weeks of age and copulation was confirmed by plug visualization and males removed postcoitum. On 10 and 15 days of pregnancy, mammary glands were collected for analysis. For studies related to lactation, litters were normalized to six pups at birth and mammary glands were collected on 0, 5 and 10 days after delivery. For studies related to involution, pups were removed on day 10 of lactation and mammary glands were collected on day 1, 2, 3, 4 and 8 after the removal of the pups.

Generation of Dnmt1 null mice

We used Cre/loxP system to conditionally delete Dnmt1 in mammary epithelial cells. $Dnmt1^{fl/fl}$ mice with loxP sites flanking exons 4 and 5 of the Dnmt1 gene, which obtained from Mutant Mouse Regional Resource Center (MMRRC) at the University of California at Davis (B6.129S4-$Dnmt1tm^{2Jae}$/Mmucd, Stock #014114-UCD, Order #146687086), was crossed into MMTV-Cre mice expressing Cre recombinase, which obtained from Jackson laboratories (Stock #003553), and generated wild-type ($Dnmt^{fl/fl}$-Cre^{-} or $Dnmt^{fl/fl}$) and Dnmt1-knockout ($Dnmt^{fl/fl}$-Cre^{+} or $Dnmt^{\Delta/\Delta}$) mice. To confirm deletion of Dnmt1, genomic DNA was extracted from the tail snip and the PCR genotype analysis was performed using the following primers: Dnmt1-Fwd: GGG CCA GTT GTG CTT GG. Dnmt1-Rev: CTT GGG CCT GGA TCT TGG GGA. To confirm the mammary gland specific Dnmt1-deletion, RNA and protein samples were prepared from the mammary glands of $Dnmt1^{fl/fl}$ and $Dnmt^{\Delta/\Delta}$ mice and Dnmt1 expression was analyzed by qPCR and western blot analyses using specific PCR primers and Dnmt1-antibody.

Generation of Dnmt1 null mice in MMTV-Neu-Tg and C3(1)-SV40-Tg mice background and monitoring tumor incidence

Female $Dnmt1^{\Delta/\Delta}$ mice were crossed with male MMTV-Neu-Tg mice and the resulting $Dnmt1^{fl/\Delta}$-MMTV-Neu-Tg mice were intercrossed to generate $Dnmt1^{fl/fl}$-MMTV-Neu-Tg and $Dnmt1^{\Delta/\Delta}$-MMTV-Neu-Tg mice. Similarly, female $Dnmt1^{\Delta/\Delta}$ mice were crossed with male C3(1)-SV40-Tg mice and the resulting $Dnmt1^{fl/\Delta}$-C3(1)-SV40-Tg mice were intercrossed to generate $Dnmt1^{fl/fl}$-C3(1)-SV40-Tg and $Dnmt1^{\Delta/\Delta}$-C3(1)-SV40-Tg mice. All the littermates generated in this study are in mixed genetic background ($Dnmt1^{fl/fl}$ mouse was in C57BL/6, MMTV-Cre mouse was in C57BL/6×129/Sv and MMTV-Neu-Tg and C3(1)-SV40-Tg mice were in FVB/N genetic background). We used 8 mice per group and repeated the experiment 3 times, thus giving 24 mice in each group. We monitored time of tumor appearance, tumor size, the number of tumors, and time and percent of lung metastasis in each mouse. When the mice became morbid due to increased tumor burden and/or lung metastasis, the animals were euthanized and the tumor tissues harvested. If mice did not develop tumor until 500 days of age for MMTV-Neu-Tg and 400 days for C3(1)-SV40-Tg, we considered that these mice are tumor-free.

Drug Treatment

For *in vivo* studies, we treated 12-weeks-old female MMTV-Neu-Tg mice with 5-azacytidine (5-AzaC) and sodium butyrate (But), either alone or in combination, by implanting the respective slow-release pellets (Innovative Research of America) in the back neck region of the animal. We established this experimental procedure recently[40]. These

pellets provided a sustained release of 5-AzaC (Catalog # NN-131, 0.5 mg/90 days) and But (Catalog # NF-125 10mg/90 days) for 90 days.

Mammary gland single cell preparation

Mammary gland single cell preparation was carried out as described previously[41]. Briefly, the thoracic and inguinal mammary glands were dissected from virgin and pregnant mice of wild-type, Dnmt1-knockout, MMTV-Neu-Tg, and C3(1)-SV40-Tg mice. The tissues were digested for 6–8 h at 37°C in DMEM/F12 medium supplemented with 10% FBS and 1% P/S and 750 U/ml Collagenase and 250 U/ml hyaluronidase. After this step, the organoids were collected by centrifugation and then subjected to trypsin (0.5%) and dispase (5mg/ml) treatment separately. After centrifugation, ammonium chloride was used for red blood cell lysis. All reagents were obtained from stem cells technology unless stated otherwise.

Transplantation assay and Whole mount analysis

Animals were anaesthetized using Isoflurane and surgery was performed to inject cells into cleared fat area. Single cell suspension that prepared from $Dnmt1^{fl/fl}$ and $DNMT1^{\Delta/\Delta}$ mice mammary epithelial cells were implanted into the cleared fat of 3-week-old syngenic female mice. In limiting dilution assays, $1\times10^2 - 1\times10^5$ mammary cells per fat pad were transplanted and the outgrowths were analyzed after 6 weeks of transplantation. Mammary repopulating unit (MRU) frequency was calculated using the online Extreme Limiting Dilution Analysis software. Dissected mammary fat pads were spread onto glass slides, fixed in a 1:3:6 mixture of acetic acid/chloroform/methanol overnight and stained with Carmine in whole mount for 12–18 hours.

Flow Cytometry

For isolation of stem/progenitor cells, the following antibodies were used: CD49f and CD24 (Stem cell technology, eBioscience), CD45 and CD31 (BD bioscience), CD44 and ISL1 (BD bioscience), and Ter119 and CD61 (eBioscience). Blocking was done for 10 min with rat serum. Cells were stained for 30 min on ice and washed with staining media. Finally, cells were resuspended in staining media containing 7-aminoactinomycin D (1 μg/ml) or 4'-6-diamidino-2-phenylindole (DAPI, 1 μg/ml) to stain dead cells. Cells were analyzed using a LSR II, Flow-jo, and sorted Mo flow cell sorter. For flow cytometric analysis of ISL1 protein expression, CAL51-pCDH and CAL51-ISL1 stable cell lines and HBL-100, MCF10A, MDAMBA231, and MDAMB436 cells were fixed with BD Cytofix fixation buffer and permeablized with BD Phosflow perm buffer. Isl1-PE (BD Bioscience) conjugated antibody was used.

DNMT and HDAC activity assay

A commercially available DNA methyltransfeases (DNMTs) assay kit (Epigentek, Farmingdale, NY, USA) was used to determine DNMT enzymatic activity as per the manufacturer's instruction. Similarly, HDAC activity was measured using the commercially available HDAC assay kit (BioVision, CA, USA) as per the manufacturer's instruction. Nuclear fractions from the mammary glands of control, 5-Azacytidine (5-AzaC), butyrate

(But) and the combination of these two (5-AzaC+But) were prepared and used as the source of DNMT and HDAC activities.

Cell culture

Human immortalized normal mammary epithelial cell lines MCF10A, obtained from ATCC (Manassas, VA) and HBL100 was kindly provided by Dr. S. Sukumar (Johns Hopkins University, Baltimore, MD). Human breast cancer cell lines (MCF7, T47D, ZR75.1, BT474, MDAMB361, MDAMB231, MDAMB453, MDAMB468 and BT20) were obtained from ATCC (Manassas, VA). CAL51 cell line was obtained from DSMZ (Braunschweig, Germany). The MCF10A cells were grown in MEGM complete medium. HBL100 cells was grown in McCoy 5A with 10% FBS. MCF7 and BT20 cells were grown in DMEM medium with 10% FBS. T47D, ZR75.1, and BT474 cells were grown in RPMI 1640 medium with 10% FBS. MDAMB231, MDAMB453, and MDAMB468 cells were grown in Leibovit's L-15 medium with 10% FBS. CAL51 cell line was grown in DMEM medium with supplemented 20% FBS. All these cell lines have been routinely tested for mycoplasma contamination using the Universal mycoplasma detection kit obtained from ATCC (Manassas, VA) and the last mycoplasma test was performed in February 2013. Mycoplasma-free cell lines were used in all of our experiments.

Generation of mammosphere

For mammosphere culture, cells were seeded in ultra-low attachment plate in DMEM/F12 medium containing B-27 supplement, bFGF, rhEGF, heparin and Penicillin/Streptomycin[42]. For matrigel culture, cells were seeded on 6 well-precoated matrigel plates and after 30 minute 10% matrigel with DMEM medium containing supplements were added. For passaging of primary spheres to secondary spheres, trypsin 0.5% along with EDTA was used. Mammospheres were disaggregated with 25 G needle. To make single cell suspension dispase (5mg/ml) used and cells filtered through 40um filter. Then cells were centrifuged at 500 g for 5 minutes and supernatant was discarded. Cells were again resuspended in mammopshere suspension media and cell numbers were counted using the haemocytometer. If single cell suspension has not been achieved, cells were again disaggregated through 25 G needle.

Cell scratch assay and analysis of apoptosis

For cell scratch assay, CAL51-pCDH and CAL51-ISL1 cells were allowed to reach 80% confluence and then serum starved for 24 hours. Cells were trypsinized and seeded into Poly lysine coated 6-well plates and allowed to adhere and spread on the substrate completely. Cells were scratched using a 200 μl pipette tip. The culture medium then was changed to standard DMEM with 20% FBS and 1% P/S. Cells were incubated at 37°C for 12 hours and Images were taken. For apoptosis assay, cells were stained with Annexin V and 7-AAD and analyzed by flow cytometer according to the manufacturer instruction (BD Bioscience).

RNA and DNA isolation and real-time PCR

Total RNA was prepared using the pure link RNA Isolation Kit (Invitrogen) or Trizol (Invitrogen). DNA was isolated using the DNeasy Blood and tissue isolation kit according to

manufacturer's protocol (Qiagen). The quality and concentration of RNA and DNA was determined by Agilent Bioanalyzer/Nano Drop Spectrometer. Isolated and purified total RNA was reverse transcribed by cDNA synthesis kit (Invitrogen). Taqman and CT kit was used for real time expression from the sorted cells. Real time PCR primers, DNMT1 (Mm01151063_m1), and HPRT (Mm01545399_m1), were designed either from applied biosystem site or Harward primer bank site (β-casein, ID1, ID2 and 18s).

Clonogenic assays

Clonogenic assay was performed as described previously[41]. Briefly, CAL51-pCDH and CAL51-ISL1 cells were seeded in 6-well plates at 1×10^3 cells/well. Cells were cultured for 2 weeks, changing the medium every 3 days, and then washed with PBS and fixed in 100% methanol for 30 min followed by staining with KaryoMax Giemsa stain for 1 h. The wells were washed with water and dried overnight at room temperature. Finally, cells were lysed with 1% SDS in 0.2 N NaOH for 5 min and the absorbance of the released dye was measured at 630 nm.

Generation of ISL1-pCDH expressing stable cell lines

Human ISL1 cDNA, which obtained from Sino Biological Inc., was subcloned into pCDH-CMV-MCS-EF1-Puro vector (System Biosciences, Mountain View, CA) at BamH1/Xba1 site. The resultant plasmid was sequenced to confirm the authenticity of the insert. Recombinant lentivirus was produced by co-transfection into 293FT cells with pCDH and ISL1-pCDH constructs and three other helper vectors, pLP-1, pLP-2, and pVSVG (Invitrogen), using Lipofectamine-2000 transfection reagent. Lentiviral supernatants were harvested at 72 h post-transfection and filtered through a 0.45-μm membrane. CAL51 cells were infected for 48 h with fresh lentivirus expressing either pCDH vector control or ISL1-pCDH construct in medium containing 8 μg/ml polybrene, and cultured for an additional 48 h. The cells were selected for puromycin resistance (4 μg/ml) for 1 week, and maintained in medium containing 1 μg/ml puromycin. The level of ISL1 mRNA expression in CAL51 cells expressing pCDH and ISL1-pCDH constructs were analyzed by qPCR. ISL1 protein expression was assessed by FACS and Western blot with an antibody specific for ISL1.

Western blot analysis

Fifty μg of the cell lystate was resolved in 8% SDS- PAGE and transferred to Nitrocellulose membranes. Membranes were incubated with primary (overnight at 4°C) and secondary (1 h at room temperature) antibodies; unbound antibodies were removed by washing the membrane with 1×TBST. Primary antibodies [DNMT1 (Cell Signaling 1:1000), ISL1 (BD Bioscience 1:5000), and β-actin (Sigma 1:25,000)] and respective secondary antibodies (Promega 1:10,000 – 1:50, 0000), were used and visualized using ECL detection system (Thermo Scientific).

Immunofluorescence staining and microscopic imaging

Seven-micron thick mammary gland/tumor sections were fixed in 4% paraformaldehyde/ methanol at room temperature for 10–15 min, washed 3 times in PBS and then blocked and permeablized in 10% goat serum, 0.1% Triton X-100 for 1 h. Sections were then incubated

in primary antibody overnight at 4°C, washed in PBS, incubated for 1 h in secondary antibodies, washed in PBST, and then mounted in Prolong gold antifade (Invitrogen) solution. Sorted cells were cytospin at 400×RPM onto Superfrost/Plus slides (Fisher), allowed to air dry, rinsed in PBS, and then stored in −80°C. For surface staining experiments, cells were fixed in 4% PFA (Electron Microscopy Sciences), whereas for nuclear staining experiment (DNMT1) cytospin cells were directly fixed in ethanol. After blocking (1 h in 10% goat serum at room temperature) slides were incubated with primary antibodies (overnight at 4°C), washed and then hybridized with secondary antibodies (1 h at room temperature), washed and mounted in Prolong Gold. Antibodies used were DNMT1 (Cell signaling, 1:250), 5meC (N81, Calbiochem) and CD49f (GoH3, R&D, 1:250), Secondary antibodies were purchased from Molecular Probes/Invitrogen: anti-rat/rabbit/mouse Alexa fluor 488 and 568 (1:1500). All sections were imaged using Laser Scanning confocal microscope. For the quantification of 5mC positive cells, pictures were taken in 6 different locations and manually counted the positive cells. Data are represented as mean ± SEM of three independent mouse sections.

Bisulfite sequencing and data analyses

"Reduced representation bisulfite sequencing (RRBS)" and analysis were performed according to a previously published protocol[43]. Briefly, raw sequences were cleaned using in-house scripts and mapped to the mouse genome release mm9 in the UCSC genome browser using Bowtie after *in silico* conversion. The methylation of each CpG was measured to determine the fraction of the number of methylated CpGs. Similarly, we measured the methylation of non-overlapping windows of 200bp. We filtered out windows that have less than 5 CpGs. For each window, the methylation difference between normal and tumor groups were calculated by the difference between the average methylation of each group. We used the student's t-test for statistical analysis. Multiple testing correction based on FDR generated adjust p-values using a function p adjust in R. DMRs (Differentially Methylated Regions) were defined as windows with an adjusted p-value < 0.05 and methylation difference > 0.25. All DMRs identified were compared using in-house scripts to RefSeq genes, CpG islands, and repeats in the UCSC genome browser and classified into functional categories. The correlation of genome-wide methylation of CpGs common in two samples was calculated by the Pearson's product-moment coefficient using an R script.

ChIP-Seq data analysis

Sequence reads were mapped to the mouse genome (mm9) using Bowtie, and only those reads that mapped to unique genomic locations with at most two mismatches were retained for further analysis. For visualization on the UCSC Genome Browser, and generation of screenshots and read density plots, the data was normalized to reads per million (RPM) and plotted as histograms. DMRs were assigned to the nearest genes (within 50Kb; RefSeq gene annotations), and read density plots for genes associated with hypermethylated or hypomethylated DMRs in tumorspheres compared with mammospheres were plotted. Published ChIP-Seq datasets used for comparative analysis: H3K27me3 in ESCs[44], H3K4me3 in ESCs (ENCODE, GSE31039), H3K27me3 and H3K4me3 in MaSCs and luminal progenitors (LPs)[7].

Statistical analysis

p value was determined using student's t-test with two-tail distribution. Kaplan-Meier analyses (http://kmplot.com/analysis/) were used to assay group differences in tumor-free survival. TCGA data base, UCGC genome, DAVID (http://david.abcc.ncifcrf.gov) and GOBO (http://co.bmc.lu.se/gobo) were also used to study biological function. Graph pad, sigma plot and excel was used to draw figure.

Supplementary Material

Refer to Web version on PubMed Central for supplementary material.

Acknowledgements

We thank Jeanene Pihkala for Flow sorting and William King for technical assistance. This work was supported by grants from the National Institute of Health (CA131402), Department of Defense (BC074289) and Georgia Regents University (GRU) Intramural Pilot Study grant, Start-up and Bridge funds. P.Y., S.C., and R.J., was supported by the Intramural Research Program of the NIH, National Institute of Environmental Health Sciences (1ZIAES102625).

References

1. Stingl J, et al. Purification and unique properties of mammary epithelial stem cells. Nature. 2006; 439:993–997. [PubMed: 16395311]
2. Stingl J, Raouf A, Emerman JT, Eaves CJ. Epithelial progenitors in the normal human mammary gland. Journal of mammary gland biology and neoplasia. 2005; 10:49–59. [PubMed: 15886886]
3. Visvader JE, Stingl J. Mammary stem cells and the differentiation hierarchy: current status and perspectives. Genes Dev. 2014; 28:1143–1158. [PubMed: 24888586]
4. Rios AC, Fu NY, Lindeman GJ, Visvader JE. In situ identification of bipotent stem cells in the mammary gland. Nature. 2014; 506:322–327. [PubMed: 24463516]
5. Asselin-Labat ML, et al. Control of mammary stem cell function by steroid hormone signalling. Nature. 2010; 465:798–802. [PubMed: 20383121]
6. Huang TH, Esteller M. Chromatin remodeling in mammary gland differentiation and breast tumorigenesis. Cold Spring Harbor perspectives in biology. 2010; 2:a004515. [PubMed: 20610549]
7. Pal B, et al. Global changes in the mammary epigenome are induced by hormonal cues and coordinated by Ezh2. Cell reports. 2013; 3:411–426. [PubMed: 23375371]
8. Smith ZD, Meissner A. DNA methylation: roles in mammalian development. Nat Rev Genet. 2013; 14:204–220. [PubMed: 23400093]
9. Bird A. DNA methylation patterns and epigenetic memory. Genes Dev. 2002; 16:6–21. [PubMed: 11782440]
10. Okano M, Bell DW, Haber DA, Li E. DNA methyltransferases Dnmt3a and Dnmt3b are essential for de novo methylation and mammalian development. Cell. 1999; 99:247–257. [PubMed: 10555141]
11. Li E, Bestor TH, Jaenisch R. Targeted mutation of the DNA methyltransferase gene results in embryonic lethality. Cell. 1992; 69:915–926. [PubMed: 1606615]
12. Tsumura A, et al. Maintenance of self-renewal ability of mouse embryonic stem cells in the absence of DNA methyltransferases Dnmt1, Dnmt3a and Dnmt3b. Genes to cells : devoted to molecular & cellular mechanisms. 2006; 11:805–814. [PubMed: 16824199]
13. Robertson KD. DNA methylation and human disease. Nat Rev Genet. 2005; 6:597–610. [PubMed: 16136652]
14. Costello JF, et al. Aberrant CpG-island methylation has non-random and tumour-type-specific patterns. Nat Genet. 2000; 24:132–138. [PubMed: 10655057]

15. Chan AO, et al. CpG island methylation in aberrant crypt foci of the colorectum. Am J Pathol. 2002; 160:1823–1830. [PubMed: 12000733]
16. Laird PW. The power and the promise of DNA methylation markers. Nat Rev Cancer. 2003; 3:253–266. [PubMed: 12671664]
17. Trowbridge JJ, Snow JW, Kim J, Orkin SH. DNA methyltransferase 1 is essential for and uniquely regulates hematopoietic stem and progenitor cells. Cell Stem Cell. 2009; 5:442–449. [PubMed: 19796624]
18. Sen GL, Reuter JA, Webster DE, Zhu L, Khavari PA. DNMT1 maintains progenitor function in self-renewing somatic tissue. Nature. 2010; 463:563–567. [PubMed: 20081831]
19. Tsai CC, Su PF, Huang YF, Yew TL, Hung SC. Oct4 and Nanog directly regulate Dnmt1 to maintain self-renewal and undifferentiated state in mesenchymal stem cells. Mol Cell. 2012; 47:169–182. [PubMed: 22795133]
20. Trowbridge JJ, et al. Haploinsufficiency of Dnmt1 impairs leukemia stem cell function through derepression of bivalent chromatin domains. Genes Dev. 2012; 26:344–349. [PubMed: 22345515]
21. Gay F, Anglade I, Gong Z, Salbert G. The LIM/homeodomain protein islet-1 modulates estrogen receptor functions. Molecular endocrinology. 2000; 14:1627–1648. [PubMed: 11043578]
22. Broske AM, et al. DNA methylation protects hematopoietic stem cell multipotency from myeloerythroid restriction. Nat Genet. 2009; 41:1207–1215. [PubMed: 19801979]
23. Tadokoro Y, Ema H, Okano M, Li E, Nakauchi H. De novo DNA methyltransferase is essential for self-renewal, but not for differentiation, in hematopoietic stem cells. J Exp Med. 2007; 204:715–722. [PubMed: 17420264]
24. Feinberg AP, Ohlsson R, Henikoff S. The epigenetic progenitor origin of human cancer. Nat Rev Genet. 2006; 7:21–33. [PubMed: 16369569]
25. Baylin SB, et al. Abnormal patterns of DNA methylation in human neoplasia: potential consequences for tumor progression. Cancer cells. 1991; 3:383–390. [PubMed: 1777359]
26. Laird PW, Jaenisch R. DNA methylation and cancer. Human molecular genetics. 1994; 3 Spec No: 1487–1495. [PubMed: 7849743]
27. Eden A, Gaudet F, Waghmare A, Jaenisch R. Chromosomal instability and tumors promoted by DNA hypomethylation. Science. 2003; 300:455. [PubMed: 12702868]
28. Herschkowitz JI, et al. Identification of conserved gene expression features between murine mammary carcinoma models and human breast tumors. Genome biology. 2007; 8:R76. [PubMed: 17493263]
29. Maroulakou IG, Anver M, Garrett L, Green JE. Prostate and mammary adenocarcinoma in transgenic mice carrying a rat C3(1) simian virus 40 large tumor antigen fusion gene. Proc Natl Acad Sci U S A. 1994; 91:11236–11240. [PubMed: 7972041]
30. Zhang W, et al. A NIK-IKKalpha module expands ErbB2-induced tumor-initiating cells by stimulating nuclear export of p27/Kip1. Cancer Cell. 2013; 23:647–659. [PubMed: 23602409]
31. Gu H, et al. Preparation of reduced representation bisulfite sequencing libraries for genome-scale DNA methylation profiling. Nature protocols. 2011; 6:468–481. [PubMed: 21412275]
32. Meissner A, et al. Genome-scale DNA methylation maps of pluripotent and differentiated cells. Nature. 2008; 454:766–770. [PubMed: 18600261]
33. Voigt P, Tee WW, Reinberg D. A double take on bivalent promoters. Genes Dev. 2013; 27:1318–1338. [PubMed: 23788621]
34. Jonsson M, Dejmek J, Bendahl PO, Andersson T. Loss of Wnt-5a protein is associated with early relapse in invasive ductal breast carcinomas. Cancer Res. 2002; 62:409–416. [PubMed: 11809689]
35. Roose J, et al. Synergy between tumor suppressor APC and the beta-catenin-Tcf4 target Tcf1. Science. 1999; 285:1923–1926. [PubMed: 10489374]
36. Latini FR, et al. ABI3 ectopic expression reduces in vitro and in vivo cell growth properties while inducing senescence. BMC Cancer. 2011; 11:11. [PubMed: 21223585]
37. Pfaff SL, Mendelsohn M, Stewart CL, Edlund T, Jessell TM. Requirement for LIM homeobox gene Isl1 in motor neuron generation reveals a motor neuron-dependent step in interneuron differentiation. Cell. 1996; 84:309–320. [PubMed: 8565076]

38. Moretti A, et al. Multipotent embryonic isl1+ progenitor cells lead to cardiac, smooth muscle, and endothelial cell diversification. Cell. 2006; 127:1151–1165. [PubMed: 17123592]

39. Gyorffy B, et al. An online survival analysis tool to rapidly assess the effect of 22,277 genes on breast cancer prognosis using microarray data of 1,809 patients. Breast Cancer Res Treat. 2010; 123:725–731. [PubMed: 20020197]

40. Elangovan S, et al. Molecular mechanism of SLC5A8 inactivation in breast cancer. Molecular and cellular biology. 2013; 33:3920–3935. [PubMed: 23918800]

41. Elangovan S, et al. The niacin/butyrate receptor GPR109A suppresses mammary tumorigenesis by inhibiting cell survival. Cancer Res. 2014; 74:1166–1178. [PubMed: 24371223]

42. Dontu G, et al. In vitro propagation and transcriptional profiling of human mammary stem/progenitor cells. Genes Dev. 2003; 17:1253–1270. [PubMed: 12756227]

43. Pei L, et al. Genome-wide DNA methylation analysis reveals novel epigenetic changes in chronic lymphocytic leukemia. Epigenetics. 2012; 7:567–578. [PubMed: 22534504]

44. Ho L, et al. esBAF facilitates pluripotency by conditioning the genome for LIF/STAT3 signalling and by regulating polycomb function. Nature cell biology. 2011; 13:903–913. [PubMed: 21785422]

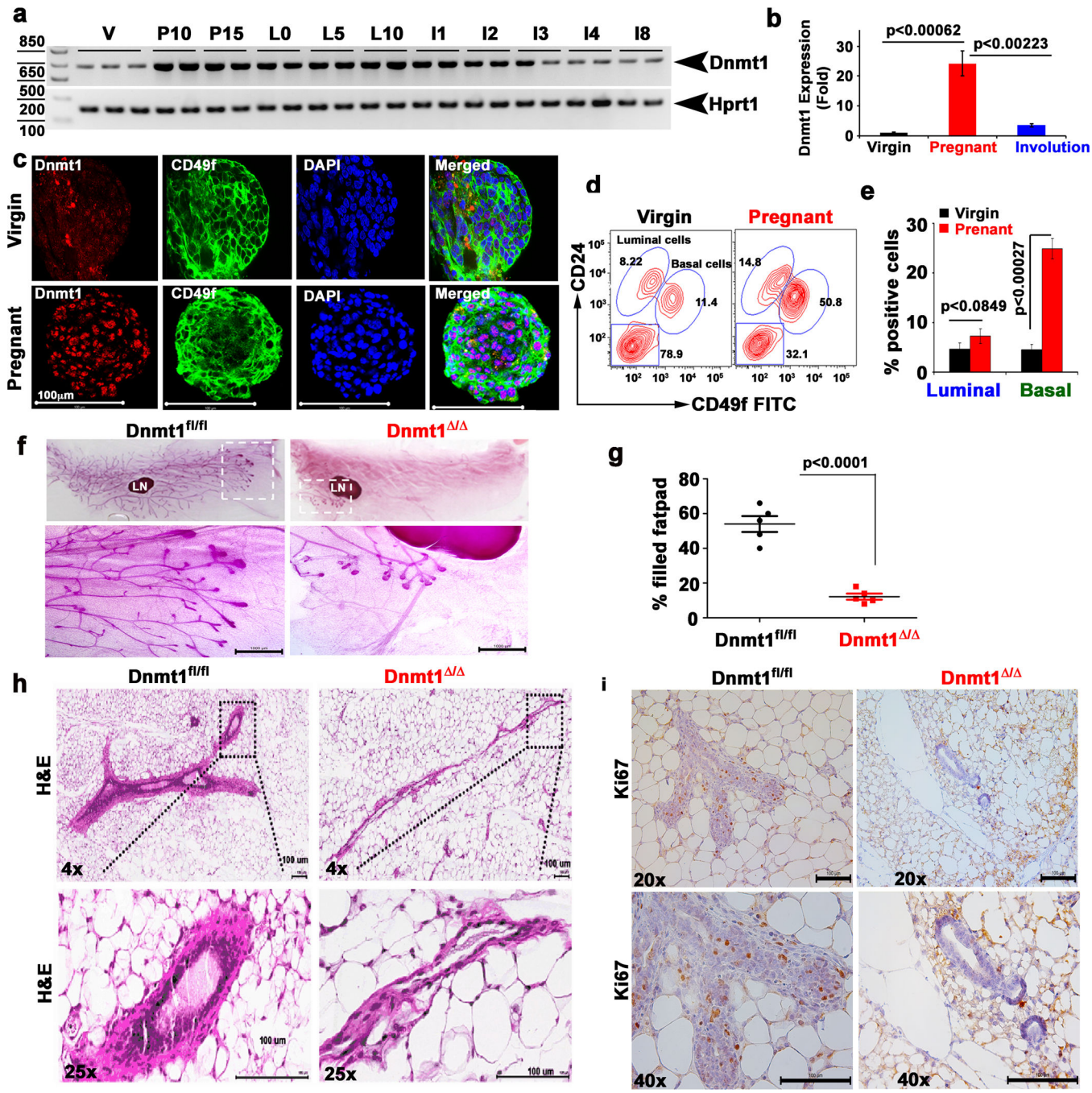

Figure 1. Dnmt1 expression during mammary gland development

a, *Dnmt1* gene transcript levels were analyzed in the mammary glands harvested from virgin (V), pregnant days 10 and 15 (P10 & P15), lactation days 0, 5 and 10 (L0, L5 & L10) and involution days 1, 2, 3, 4 and 8 (I1, I2, I3, I4 and I8) mice. Hprt1 was used as a loading control. (n=3 mice in each time point). **b**, Real time PCR showing relative expression of *Dnmt1* from virgin, pregnancy and involution stage (n=3). **c**, Representative immunofluorescence (IF) staining for Dnmt1 (red), CD49f (green) and DAPI (blue) in mammospheres generated with cells from virgin mice and pregnant mice at 10th day of

gestation (n=3). Scale bar 100 μm. **d**, Representative contour plots of FACS gating showing a 4-fold increase in basal myoepithelial stem cells in mammary glands of pregnant mice at 10^{th} day of gestation compared to mammary glands of virgin mice (n=3–5). **e**, Bar diagram showing percent positive basal and luminal cells in virgin and pregnant mice. Data represents mean ± SD of 4 independent mice in each group. **f**, Carmine staining of inguinal mammary glands from 7 weeks old wild-type (*Dnmt1*$^{fl/fl}$) and *Dnmt1*-knockout (*Dnmt1*$^{\Delta/\Delta}$) littermates shows severe delay in TEB development in *Dnmt1*-knockout mice (n=3). LN stands for lymph mode. Scale bar 100 μm. **g**, quantification for percent fat pad filled in the mammary gland (n=3). **h**, H & E image of wild-type and *Dnmt1*$^{\Delta/\Delta}$ mouse mammary gland sections show severe defect in mammary gland development. Images were taken at 4× and 20× magnifications (n=3). Scale bar 100 μm. **i**, Ki67 stained section and histogram of wild-type and *Dnmt1*$^{\Delta/\Delta}$ mammary glands show significantly reduced Ki67 staining in *Dnmt1*$^{\Delta/\Delta}$ mice. Images were taken at 20× and 40× magnifications. Scale bar 100 μm. Statistical analysis was performed using unpaired Student's *t*-tests. Error bars represent SEM of independent experiments.

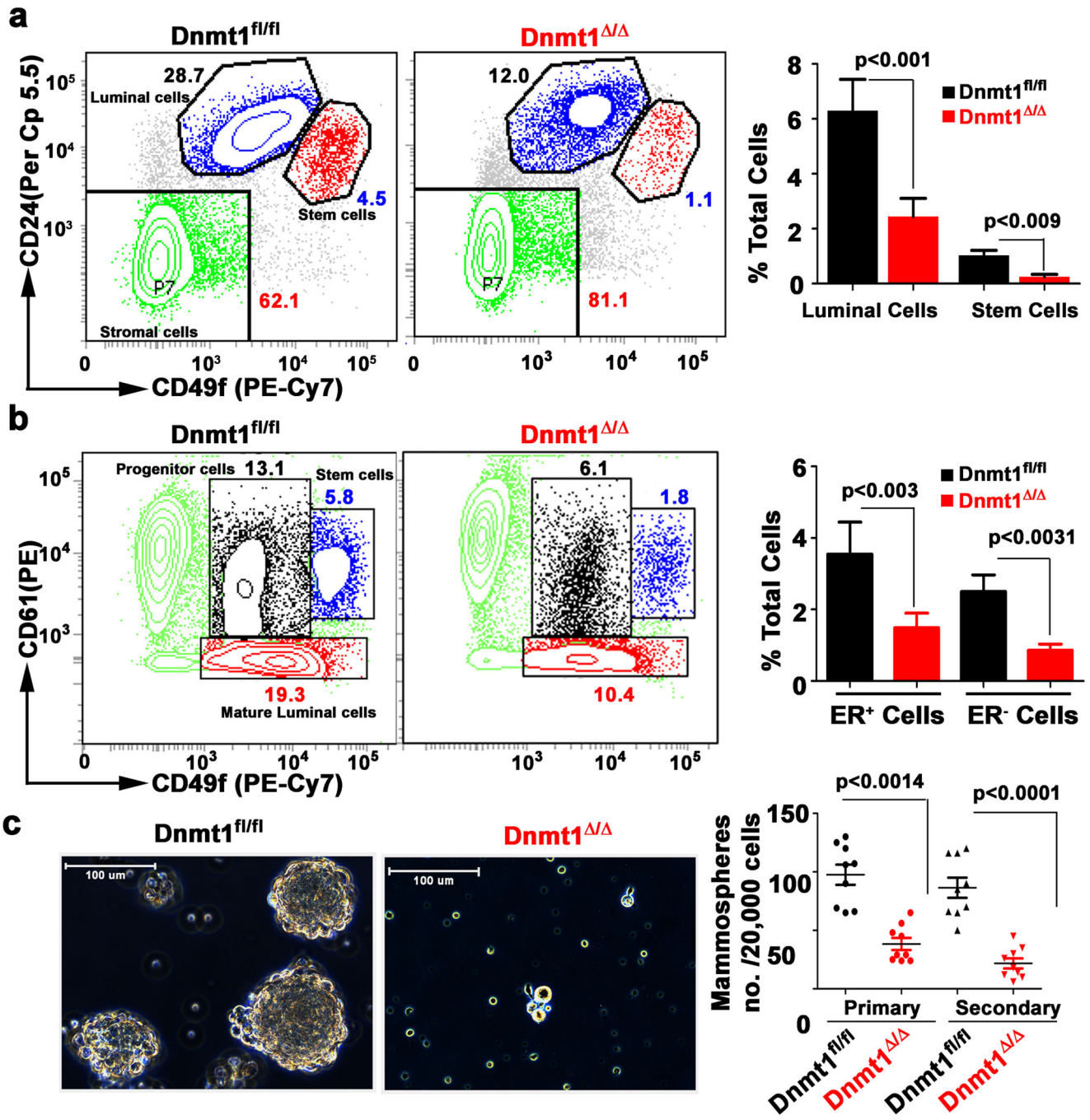

Figure 2. Dnmt1 is indispensable for mammary stem/progenitor cell maintenance

a, Single cell suspensions from mammary glands of Dnmt1$^{fl/fl}$ and Dnmt1$^{\Delta/\Delta}$ mice were stained with CD24, CD49f, and Lin (CD31, CD45 and CD119) antibodies. Representative FACS dot blots showing reduced stem (Lin^{-}CD49f^{high}CD24^{+}) and luminal cells (Lin^{-}CD49f^{low}CD24^{+}) in *Dnmt1*-knockout mice (n=3–5 mice in each). Bar diagram represents percent of total stem and luminal cell populations in the respective mammary glands. **b**, Similarly, single cell suspensions from mammary glands of *Dnmt1*$^{fl/fl}$ and *Dnmt1*$^{\Delta/\Delta}$ mice were stained with CD61, CD49f and Lin antibodies. Representative contour

blots show reduced luminal progenitor cells ($Lin^{-}CD49f^{low}CD61^{+}$) in *Dnmt1*-knockout mice. Bar diagram represents percent of total ER^{+} and ER^{-} cell populations in the respective mammary glands. **c**, Representative images show a decrease in size and number in mammospheres generated with cells from *Dnmt1*$^{\Delta/\Delta}$ mice compared with cells from $Dnmt1^{fl/fl}$ mice (n=3–5). 20,000 cells/ml were used in each group. Bar diagram represents total number of mammospheres per 20,000 cells. Scale bar 100 μm. Data are representative of 5 independent mice per group. Statistical analysis was performed using unpaired Student's *t*-tests. Error bards represent SEM of independent experiments.

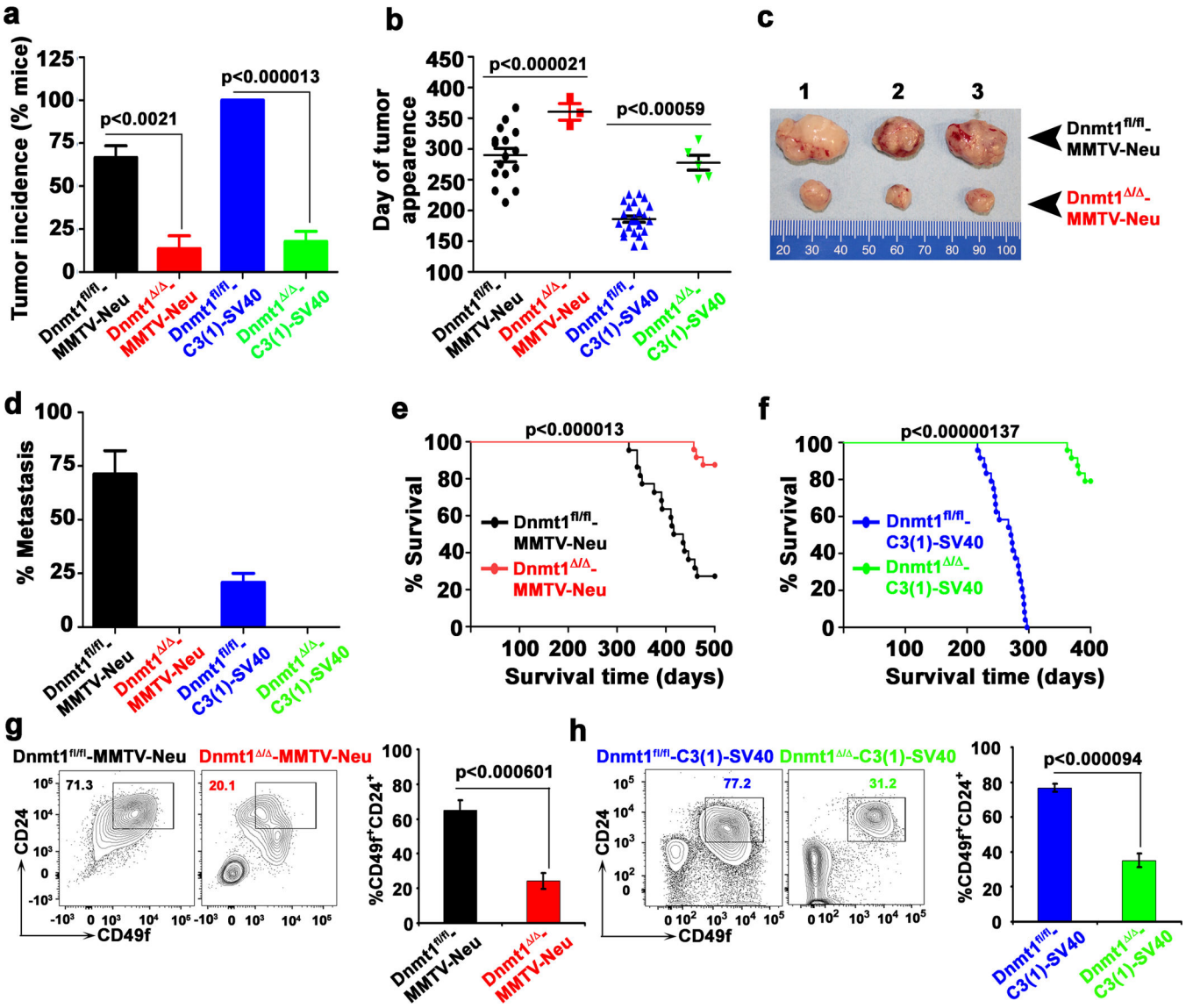

Figure 3. *Dnmt1* deletion suppresses mammary tumorigenesis

Dnmt1$^{\Delta/\Delta}$ mice were crossed with MMTV-Neu-Tg and C3(1)-SV40-Tg mice to generate MMTV-Neu and C3(1)-SV40 transgenic mice in wild-type and *Dnmt1*-null genetic backgrounds. Using these mice, we monitored **a**, tumor incidence, **b**, age of the animals at tumor onset, **c**, tumor size, **d**, lung metastasis, and **e, f**, average survival time. Data are mean ± SEM (n= 24 mice in each group). **g–h**, Representative contour blots show reduced cancer stem cells (CSC, CD49f^{+}CD24^{+}) in Dnmt1$^{\Delta/\Delta}$-MMTV-Neu and Dnmt1$^{\Delta/\Delta}$-C3(1)-SV40 mice compared to their respective controls. Bar diagrams represent percent cancer stem cell populations of respective mouse mammary tumors. Data are mean ± SEM (n= 5 mice in each group). Statistical analysis was performed using unpaired Student's *t*-tests. Error bards represent SEM of independent experiments.

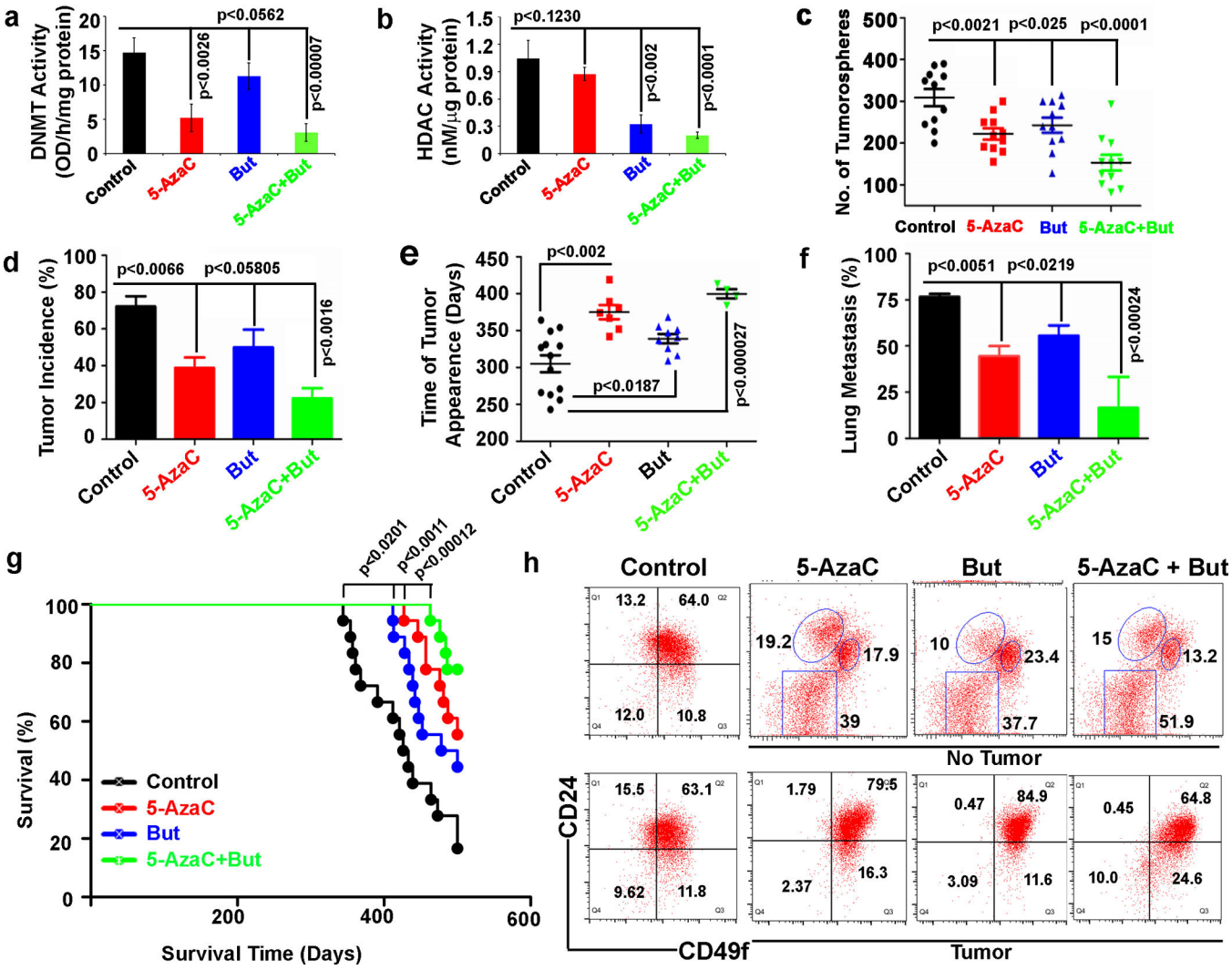

Figure 4. Inhibition of DNMT activity suppresses mammary tumorigenesis

a, DNA methyl transferase (DNMTs) activity was measured in the nuclear extracts prepared from the mammary tumor tissues of untreated control, 5-AzaC, But and the combination (5-AzaC+But). **b**, Histone deacetylases activity (HDAC) was measured from the nuclear extract of mammary tumor tissues of untreated control, 5-AzaC, But and the combination (5-AzaC+But). Data represent mean ± SD of 6 mice in each group. **c**, Tumorospheres number in untreated control, 5-AzaC, But and the combination (5-AzaC+But). Data represent mean ± SD of three independent experiments. **d–g**, Prophylactic treatment of 5-azacytidine (5-AzaC), But and combination (5-AzaC+But) in MMTV-Neu-Tg mice reduced tumor incidence, delayed tumor growth, lung metastasis with increased overall survival. Data represent mean ± SD of n=18 mice per group. **h**, Representative FACS dot plot for the untreated control, 5-azaC, But and combination (5-AzaC+But) in MMTV-Neu-Tg mice. Top rows represent the mammary tissues with no visible tumor upon treatment with 5-AzaC, But and combination (5-AzaC+But) in MMTV-Neu-Tg mice. Bottom rows represent visible tumors tissues upon treatment with 5-AzaC, But and combination (5-AzaC+But) in MMTV-Neu-Tg mice. Statistical analysis was performed using unpaired Student's *t*-tests.

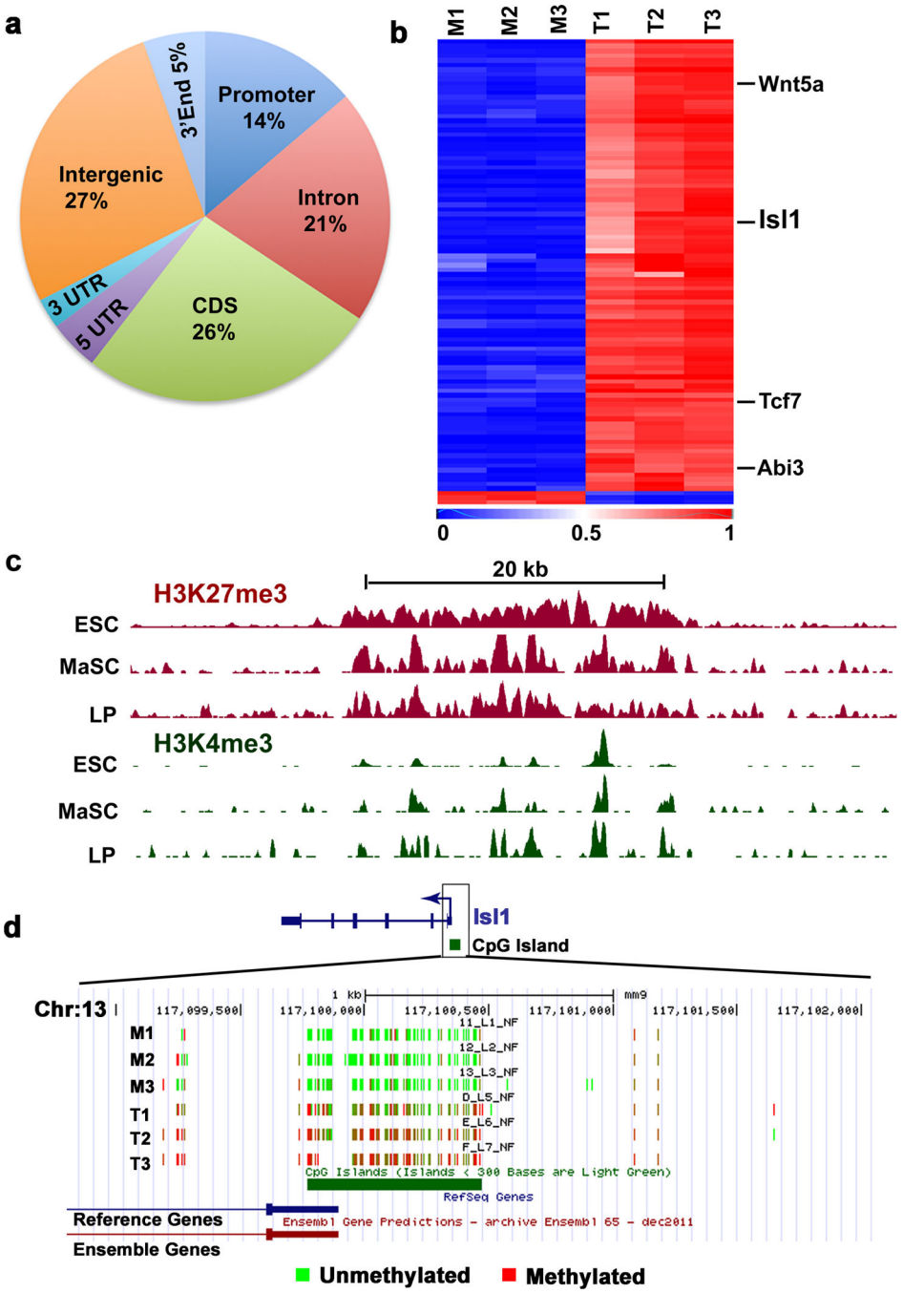

Figure 5. ***Isl1*** **is hypermethylated in mammary tumors**

a, Genome-scale distribution of DMRs identified in mammospheres of normal mammary stem cells and tumorospheres of tumor-initiating cells prepared from MMTV-Neu-Tg mice (n=3 mice in each). **b**, Cluster analysis of top 100 hypermethylated and few hypomethylated genes. c, Genome browser shot showing ChIP-Seq tracks for H3K27me3 (red) and H3K4me3 (green) levels near *Isl1* in embryonic stem cells (ESCs), MaSCs, and luminal progenitors (LPs). **d**, UCSC genome browser screenshot showing DNA methylation profile

at ISL1 locus in mammospheres and tumorospheres. Red and green colors indicate methylated and unmethylated CpG sites, respectively.

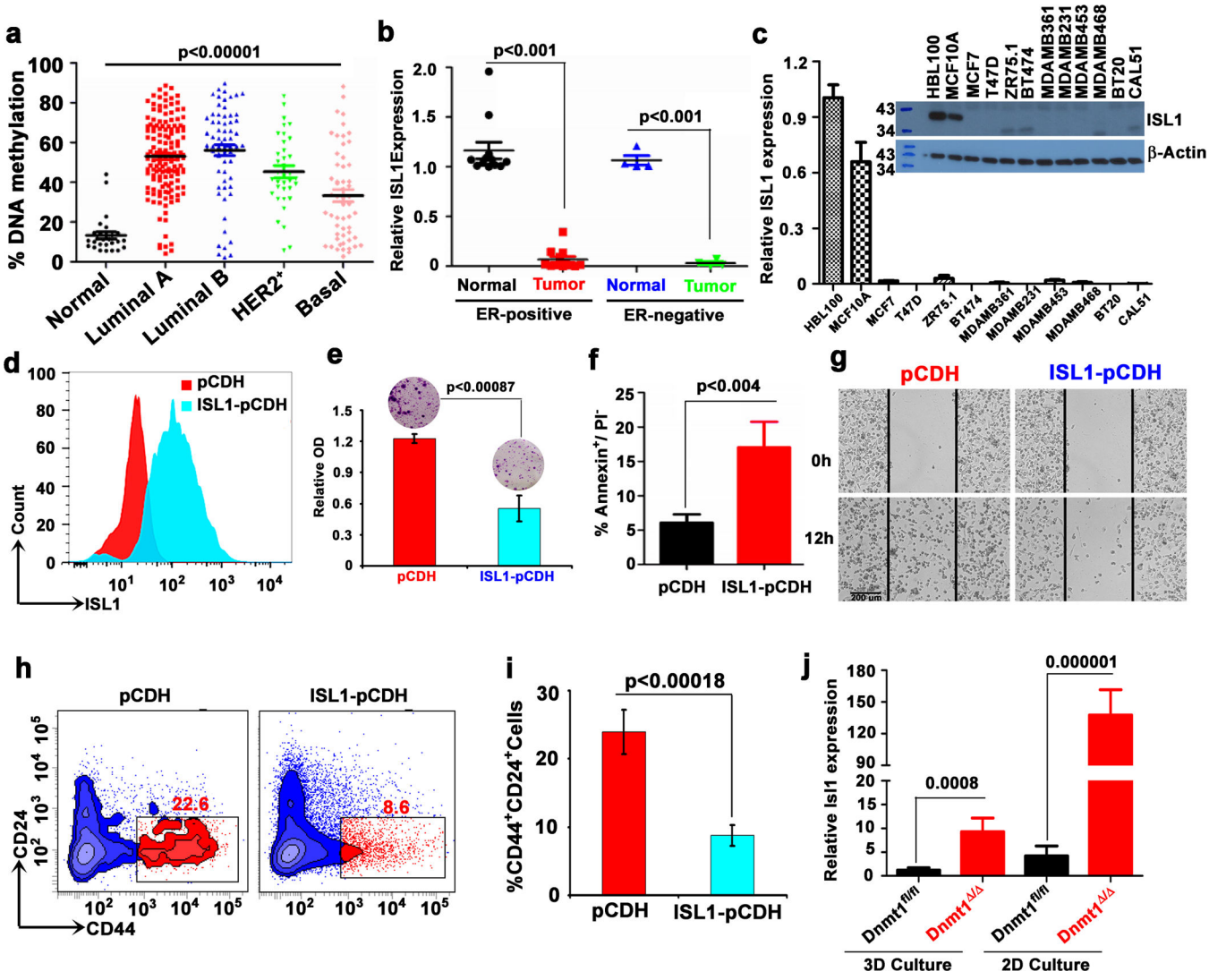

Figure 6. ISL1 expression in cancer cells limits CSC population

a, *ISL1* promoter was analyzed from TCGA human methylation 27K methylation dataset at a single CpG site (cg21410991) for differential methylation in luminal A, luminal B, HER2-Neu, and basal breast cancer subtypes. **b**, *ISL1* expression in ER-positive (n=12) and negative (n=4) breast tumor and respective normal breast tissues show reduced expression of this gene in both tumor subtypes. **c**, ISL1 expression in human non-transformed normal mammary epithelial and human breast cancer cell lines was analyzed by qPCR and western blot analysis. **d**, Representative FACS data confirming exogenous expression of ISL1 in CAL51 cell line. **e**, Representative images of colony formation assay of CAL51-pCDH and CAL51-ISL1 stable cell lines show that ISL1 expression significantly reduces colony formation. The resulting colonies were stained with Giemsa dye and bound Giemsa dye were dissolved and quantified by spectrophotometer analysis. Data represents mean ± SD from three independent experiments. **f**, Histogram shows that ISL1 expression in CAL51 cells increased apoptosis (Annexin V^+/PI^-) compared to vector control. Data are mean ± SEM of 3 independent experiments. **g**, CAL51-pCDH and CAL51-ISL1 expressing stable

cells were subjected to *in vitro* scratch assay and images were captured using phase-contrast microscope at 12 h after incubation. Scale bar 200 μm. **h**, Representative FACS plot shows decreased cancer stem cells ($CD44^{+}CD24^{-}$) in ISL1 expressing CAL51 cells. **i**, Histogram showing percent decrease in cancer stem cells after ISL1 expression in CAL51 cells. **j**, Relative *ISL1* expression in wild-type and *DNMT1*-null mice after 3D and 2D culture. (n=3 mice). Statistical analysis was performed using unpaired Student's *t*-tests.

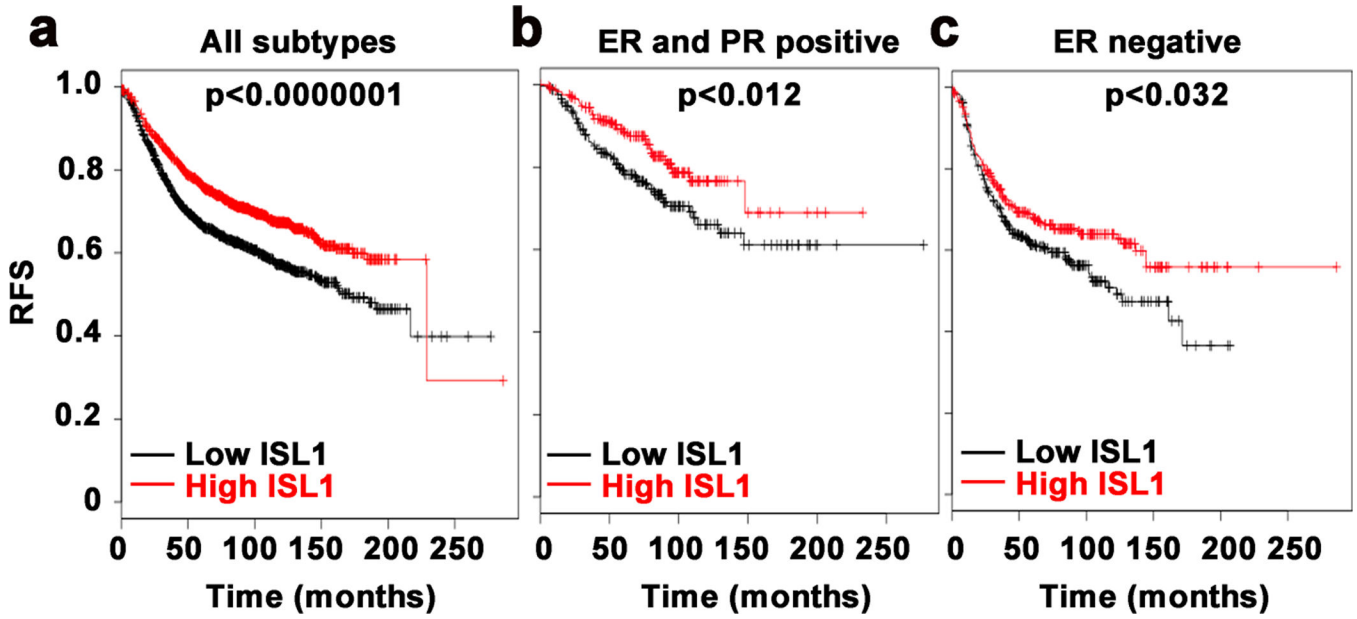

Figure 7. Association between ISL1 expression and overall survival

Kaplan-Meier plots of overall survival of breast cancer patients in whole data sets for all breast cancer patients (**a**), estrogen receptor positive and progesterone receptor positive patients (**b**), and estrogen receptor negative patients (**c**), stratified by ISL1 expression. Data were obtained from the Kaplan-Meier plotter breast cancer survival analysis database. The p value was calculated using a log rank test.